

Diarylnitroxide Diradicals: Low-Temperature Oxidation of Diarylamines to Nitroxides

Andrzej Rajca,* Matthew Vale, and Suchada Rajca

Department of Chemistry, University of Nebraska, Lincoln, Nebraska 68588-0304

Received March 4, 2008; E-mail: arajca1@unl.edu

Abstract: A low temperature method, in which the progress of the oxidation of secondary diarylamines with DMDO at low temperatures is monitored by magnetic resonance spectroscopy (EPR and NMR) and magnetic studies by a Superconducting Quantum Interference Device (SQUID), is developed for preparation of the first *m*-phenylene based diarylnitroxide diradical. EPR spectroscopy and magnetic studies (SQUID) indicate that the diradical in the dichloromethane matrix predominantly adopts anticonformation (**2A-anti**) and possesses triplet ground state. Similar oxidation experiments for conformationally constrained aza[1₄]metacyclophane provide evidence for the formation of small amounts of the corresponding diarylnitroxide diradical. Both diarylnitroxide diradicals could only be detected at low temperatures (−80 °C and below).

1. Introduction

Nitroxides are among the most widely used stable radicals in chemistry and biology.^{1–4} One of the important applications is in materials chemistry, in which nitroxides have been used as building blocks for organic magnetic materials.^{5,6} The general designs of such organic magnets have been based upon intermolecular ferromagnetic interactions between the radicals in the solid state. The first organic ferromagnet, β -polymorph of the 4-nitrophenyl nitronyl nitroxide, was reported by Kinoshita and co-workers in 1991,⁷ and there have been several reports of organic ferromagnets since then.^{8–10} It is important to note that the nitroxide-based ferromagnets have magnetic ordering at very low temperatures, below 2 K, which is limited

by the intrinsic weakness of intermolecular interactions between the neutral radicals.^{7,8,11}

Another approach to organic materials with magnetic ordering has been based on macromolecules with intramolecular ferromagnetic interactions between organic radicals (high-spin polyradicals).^{12–14} In this approach, the intrinsic strength of intramolecular ferromagnetic interactions mediated through a cross-conjugated π -system shows promise for magnetic ordering at relatively high temperatures, significantly exceeding the temperature of about 10 K.¹⁵ An example of this approach is the first organic polymer with magnetic ordering reported in 2001.¹⁶ Because *m*-phenylene has been shown to be one of the most effective spin coupling units,^{17–19} the building blocks consisting of nitroxides coupled through the *m*-phenylenes are highly promising for preparation of organic magnetic materials.²⁰

To date, there are only relatively few known stable diarylnitroxide radicals in which nitroxide is connected to two aryl

- (1) Hawker, C. J.; Bosman, A. W.; Harth, E. *Chem. Rev.* **2001**, *101*, 3661–3688.
- (2) Shibuya, M.; Tomizawa, M.; Suzuki, I.; Iwabuchi, Y. *J. Am. Chem. Soc.* **2006**, *128*, 8412–8413.
- (3) Chernick, E. T.; Mi, Q.; Kelley, R. F.; Weiss, E. A.; Jones, B. A.; Marks, T. J.; Ratner, M. A.; Wasielewski, M. R. *J. Am. Chem. Soc.* **2006**, *128*, 4356–4364.
- (4) Soule, B. P.; Hyodo, F.; Matsumoto, K.-I.; Simone, N. L.; Cook, J. A.; Krishna, M. C.; Mitchell, J. B. *Free Radical Biol. Med.* **2007**, *42*, 1632–1650.
- (5) Kinoshita, M. Magnetism of Stable Organic Radical Crystals. In *Handbook of Organic Conductive Molecules and Polymers*; Nalwa, H. S., Ed.; Wiley: New York, 1997; Chapter 15, pp 781–800.
- (6) Itoh, K.; Kinoshita, M. Eds.; *Molecular Magnetism, New Magnetic Materials*; Gordon and Breach: Amsterdam, 2000; pp 1–337.
- (7) Tamura, M.; Nakazawa, Y.; Shiomi, D.; Nozawa, K.; Hosokoshi, Y.; Ishikawa, M.; Takahashi, M.; Kinoshita, M. *Chem. Phys. Lett.* **1991**, *186*, 401–403.
- (8) Chiarelli, R.; Novak, M. A.; Rassat, A.; Tholence, J. L. *Nature* **1993**, *363*, 147–149.
- (9) (a) Fullerene radical cation salt is a ferromagnet with magnetic ordering at 16 K. Allemand, P.-M.; Khemani, K. C.; Koch, A.; Wudl, F.; Holczer, K.; Donovan, S.; Gruner, G.; Thompson, J. D. *Science* **1991**, *253*, 301–303. (b) Narymbetov, B.; Omerzu, A.; Kabanov, V. V.; Tokumoto, M.; Kobayashi, H.; Mihailovic, D. *Nature* **2000**, *407*, 883–885.
- (10) Alberola, A.; Less, R. J.; Pask, C. M.; Rawson, J. M.; Palacio, F.; Olliete, P.; Paulsen, C.; Yamaguchi, A.; Farley, R. D.; Murphy, D. M. *Angew. Chem., Int. Ed.* **2003**, *42*, 4782–4785.

- (11) Intermolecular antiferromagnetic interactions, which can be relatively strong, can lead to magnetic ordering in the presence of significant magnetic anisotropy at temperatures as high as 36 K but providing materials with very small magnetic moments (“weak ferromagnets”) Banister, A. J.; Bricklebank, N.; Lavender, I.; Rawson, J. M.; Gregory, C. I.; Tanner, B. K.; Clegg, W.; Elsegood, M. R. J.; Palacio, F. *Angew. Chem., Int. Ed. Engl.* **1996**, *35*, 2533–2535.
- (12) Rajca, A. *Chem. Rev.* **1994**, *94*, 871–893.
- (13) Rajca, A.; Wongsriratanakul, J.; Rajca, S. *J. Am. Chem. Soc.* **2004**, *126*, 6608–6626.
- (14) Fukuzaki, E.; Nishide, H. *J. Am. Chem. Soc.* **2006**, *128*, 996–1001.
- (15) Rajca, A. *Chem.-Eur. J.* **2002**, *8*, 4834–4841.
- (16) Rajca, A.; Wongsriratanakul, J.; Rajca, S. *Science* **2001**, *294*, 1503–1505.
- (17) Fang, S.; Lee, M.-S.; Hrovat, D. A.; Borden, W. A. *J. Am. Chem. Soc.* **1995**, *117*, 6727–6731.
- (18) Wenthold, P. G.; Kim, J. B.; Lineberger, W. C. *J. Am. Chem. Soc.* **1997**, *119*, 1354–1359.
- (19) Wang, T.; Krylov, A. I. *J. Chem. Phys.* **2005**, *123*, 104304–1104304–6.
- (20) Rajca, A.; Takahashi, M.; Pink, M.; Spagnol, G.; Rajca, S. *J. Am. Chem. Soc.* **2007**, *129*, 10159–10170.

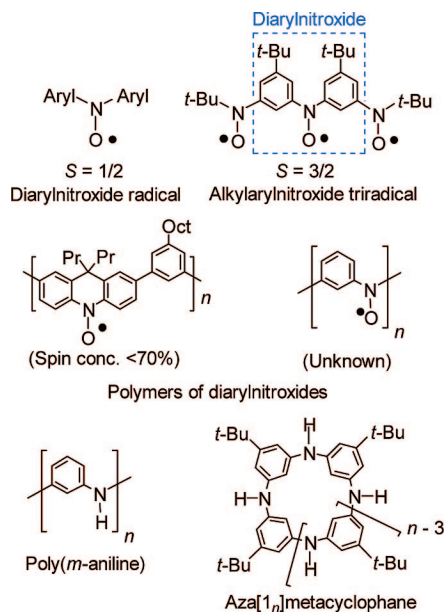


Figure 1. Diarylnitroxide radicals and secondary diarylamines.

groups.^{21–24} Delocalization of spin density to aryl groups allows, in principle, for the design of extended high-spin polyradicals based upon cross-conjugation of nitroxide radicals.¹⁵ On the basis of this design, the diarylnitroxide moiety was connected to two *tert*-butylnitroxides (Figure 1), nitronyl nitroxides, and imino nitroxides, to provide quartet ($S = 3/2$) ground-state nitroxide triradicals.^{25,26} Although steric shielding of spin density by the *tert*-butyl groups at the meta positions with respect to the nitroxides is sufficient for stability of triradicals at ambient conditions, there is no report of polyradicals based on this approach.^{25,26} A polymer of diarylnitroxide radicals was reported, though the reported concentration of radicals was modest (Figure 1).²⁷ In this polymer, nitroxides were cross-conjugated by terphenylene groups, which provided a long exchange pathway leading to a very weak ferromagnetic exchange coupling.²⁷

It is well-established that cross-conjugation of nitroxides through *m*-phenylene could lead to a strong ferromagnetic coupling, exceeding RT at room temperature.^{17,20,28} Furthermore, it may be postulated that such nitroxide polyradicals could be prepared from poly(*m*-aniline) or its oligomers as their oxidation products (Figure 1);²⁹ however, there is no report to date of the

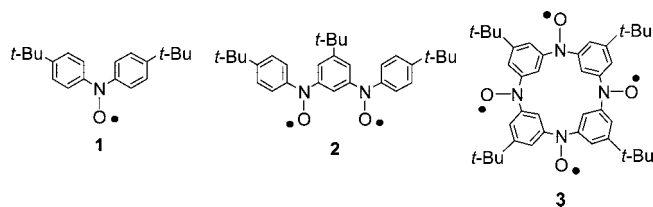


Figure 2. Diarylnitroxide radicals.

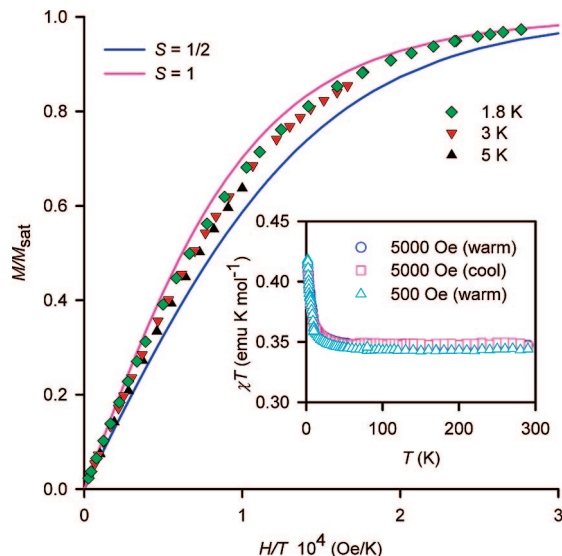


Figure 3. SQUID magnetometry for polycrystalline nitroxide radical **1**, crystallized from ethanol. Main plot: M/M_{sat} vs H/T at set temperatures of 1.8, 3, and 5 K, corresponding to $S = 0.85$, 0.80, and 0.67, respectively. Inset plot: χT vs T in the warming and cooling modes at set magnetic fields of 5000 and 500 Oe.

successful preparation of such diarylnitroxide diradicals or polyradicals.³⁰

Recently, we reported the synthesis of a series of aza[1_n]metacyclophanes that are macrocyclic oligomers of poly(*m*-aniline) (Figure 1).³¹ These structures were designed as potential building blocks for robust high-spin nitroxide polyradicals, in which we expected that the *tert*-butyl groups at the meta positions with respect to the nitroxides would provide adequate shielding to the nitroxides, analogously to those in the diarylnitroxide moiety of stable $S = 3/2$ nitroxide triradicals. Assessment of the effectiveness of this structure design will require an effective methodology for the generation of nitroxide polyradicals derived from secondary diarylpolymers.

Herein, we report the development of a methodology for the generation of diarylnitroxide radicals from secondary diarylamines. We first prepared nitroxide radical **1**²² from the corresponding diarylamine following known procedures for oxidation of secondary amines with *meta*-chloroperbenzoic acid (*m*-CPBA)²¹ and for oxidation of secondary dialkylamines with dimethyldioxirane (DMDO) to the corresponding nitroxides.³² Radical **1** is isolated as crystalline solid, stable at ambient conditions, and showing intermolecular interactions at low temperatures. However, these oxidation methods failed to

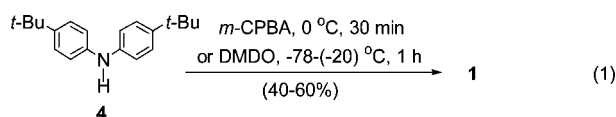
- (21) Forrester, A. R.; Hay, J. M.; Thomson, R. H. *Organic Chemistry of Stable Free Radicals*; Academic Press: London, 1968; Chapter 5, pp 180–246.
- (22) (a) Ivanov, Y. A.; Kokorin, A. I.; Shapiro, A. B.; Rozantsev, E. G. *Izv. Akad. Nauk SSSR, Ser. Khim.* **1976**, *10*, 2217–2222. (b) In the original synthesis of radical **1**, the yield of 70% from the corresponding amine, using $\text{Na}_2\text{WO}_4/\text{H}_2\text{O}_2$, was reported, though purity of **1** was not established.
- (23) Delen, Z.; Lahti, P. M. *J. Org. Chem.* **2006**, *71*, 9341–9347.
- (24) Several examples of diarylnitroxides with ferromagnetic exchange coupling in the solid state were reported, and the strength of coupling was generally weak. Seino, M.; Akui, Y.; Ishida, T.; Nogami, T. *Synth. Met.* **2003**, *133–134*, 581–583.
- (25) Ishida, T.; Iwamura, H. *J. Am. Chem. Soc.* **1991**, *113*, 4238–4241.
- (26) Tanaka, M.; Matsuda, K.; Itoh, T.; Iwamura, H. *J. Am. Chem. Soc.* **1998**, *120*, 7168–7173.
- (27) Oka, H.; Kouno, H.; Tanaka, H. *J. Mater. Chem.* **2007**, *17*, 1209–1215.
- (28) Sato, H.; Kathirvelu, V.; Spagnol, G.; Rajca, S.; Rajca, A.; Eaton, S. S.; Eaton, G. R. *J. Phys. Chem. B* **2008**, *112*, 2818–2828.
- (29) Baumgarten, M.; Müllen, K.; Tyutyulkov, N.; Madjarova, G. *Chem. Phys.* **1993**, *169*, 81–84.

- (30) Miura, Y. Synthesis and Properties of Organic Conjugated Polyradicals. In *Magnetic Properties of Organic Materials*; Lahti, P. M., Ed.; Marcel Dekker: New York, 1999; pp 267–284.
- (31) Vale, M.; Pink, M.; Rajca, S.; Rajca, A. *J. Org. Chem.* **2008**, *73*, 27–35.
- (32) Murray, R. W.; Singh, M. *Tetrahedron Lett.* **1988**, *29*, 4677–4680.

generate diarylnitroxide diradical **2**. To solve this problem, we developed an oxidation method in which the progress of the oxidation of secondary diarylamines with DMDO is monitored by magnetic resonance spectroscopy (EPR and ^1H NMR) and by magnetic studies in solution using a Superconducting Quantum Interference Device (SQUID), with the reaction mixture strictly maintained at low temperature ($-80\text{ }^\circ\text{C}$ or below). This allowed us to optimize the reaction conditions. Using this methodology, we detected for the first time an *m*-phenylene-based diarylnitroxide diradical such as **2**, and establish that this diarylnitroxide is persistent only at low temperatures ($-80\text{ }^\circ\text{C}$ or below). However, when this method was tested for the oxidation of aza[1_n]metacyclophane ($n = 4$) to tetradical **3** (Figure 2), only the corresponding nitroxide diradical was detected.

2. Results and Discussion

2.1. Oxidation of Diarylmonoamine. Oxidation of diarylamine **4** with *meta*-chloroperbenzoic acid (*m*-CPBA) or dimethyldioxirane (DMDO) produces diarylnitroxide radical **1** in 40–60% isolated yields (eq 1).^{22b}



These yields are significantly lower than the nearly quantitative yields reported for oxidation of sterically hindered secondary dialkylamines with DMDO to the corresponding dialkyl nitroxide radicals such as TEMPO.³²

EPR spectrum of dilute solution of **1** in diethyl ether or in toluene shows the expected hyperfine splittings, including ^{14}N -hyperfine splitting, $|a_{\text{N}}| = 0.97\text{ mT}$ (Figures S1A and S1B, Supporting Information).^{22a} ^1H NMR spectrum of concentrated solution of **1** in chloroform-*d* shows a broad singlet at about 6.2 ppm, which is assigned to the *tert*-butyl groups (Figure S2, Supporting Information). This chemical shift corresponds to a paramagnetic shift, $\Delta\delta_{\text{p}} = +4.9\text{ ppm}$ for protons of the *tert*-butyl groups.³³ The positive sign of $\Delta\delta_{\text{p}}$ may be ascribed to the conjugative mechanism (“homohyperconjugation”) for the transfer of positive spin density from para positions of the phenyl nitroxide to the *tert*-butyl hydrogens, as observed for 4-alkylphenyl-*tert*-butylnitroxide radicals; the value of isotropic electron–proton hyperfine splitting (a_{H} in mT) for *tert*-butyl hydrogens, $a_{\text{H}} \approx +0.006\text{ mT}$,^{20,34} is similar to those reported in 4-*tert*-butylphenyl-*tert*-butylnitroxide and 4-*tert*-butylphenyl-substituted radicals.^{35,36} The integration indicates about 10 mol% content of solvent used for crystallization and negligible amount of other diamagnetic byproduct. The purity of radical **1** is confirmed by magnetic studies using a SQUID.

(33) As a small correction for bulk paramagnetic susceptibility of the order of 0.5 ppm is not included, the actual value of $\Delta\delta_{\text{p}}$ is somewhat lower.

(34) For $S = 1/2$ nitroxide radical ($g = 2.005$) at room temperature ($T = 295\text{ K}$): a_{H} (mT) = $0.00133 \Delta\delta_{\text{p}}$.

(35) (a) The values of $a_{\text{H}} = +0.0054\text{ mT}$ and $a_{\text{H}} = +0.0059\text{ mT}$ for the protons of the *tert*-butyl group were obtained from the ^1H NMR spectra of 4-*tert*-butylphenyl-*tert*-butylnitroxide radical in chloroform-*d* and carbon tetrachloride. (b) Torsell, K.; Goldman, J.; Petersen, T. E. *Liebigs Ann. Chem.* **1973**, 231–240. (c) Forrester, A. R.; Hepburn, S. P.; McConnachie, G. J. *Chem. Soc., Perkin Trans. 1* **1974**, 2213–2219.

(36) In polyarylmethyl triradical, the ^1H -resonance at +10 ppm was assigned to the *t*-Bu groups in the 4-*tert*-butylphenyls adjacent to the radicals, suggesting analogous homohyperconjugation: Rajca, S.; Rajca, A. *J. Am. Chem. Soc.*, **1995**, *117*, 9172–9179.

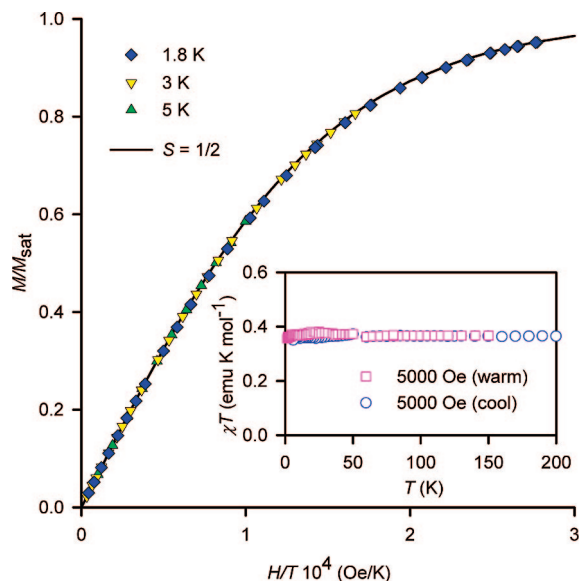


Figure 4. SQUID magnetometry for $\sim 0.1\text{ M}$ nitroxide radical **1** in 2-MeTHF. Main plot: M/M_{sat} vs H/T at set temperatures of 1.8, 3, and 5 K. Inset plot: χT vs T in the warming and cooling modes at set magnetic field of 5000 Oe.

For polycrystalline diarylnitroxide radical **1**, the plot of the product of magnetic susceptibility and temperature (χT) versus T is flat at higher temperatures ($T > 25\text{ K}$) with $\chi T = 0.35\text{ emu K mol}^{-1}$, which is nearly identical to the value of $S(S + 1)/2 = 0.375\text{ emu K mol}^{-1}$ for an $S = 1/2$ paramagnetic radical (Figure 3). Interestingly, the χT versus T plot shows an upward turn at low temperature, with $\chi T = 0.42\text{ emu K mol}^{-1}$ at 1.8 K, that is assigned to intermolecular ferromagnetic interactions.²⁴ The ferromagnetic nature of these interactions is confirmed by the increasing values of $S > 1/2$ for the Brillouin plots, M/M_{sat} versus H/T , at decreasing $T = 5, 3,$ and 1.8 K .

For **1** in 2-methyltetrahydrofuran (2-MeTHF), a near perfect $S = 1/2$ paramagnetic behavior is found, thus confirming intermolecular nature of the ferromagnetic interaction of polycrystalline radical. The χT versus T plot is flat in the $T = 2\text{--}200\text{ K}$ range and the M/M_{sat} versus H/T plot coincides with the $S = 1/2$ Brillouin curve. Both values of $\chi T = 0.37\text{ emu K mol}^{-1}$ and $M_{\text{sat}} = 0.97\text{ } \mu_{\text{B}}$ are nearly identical to those expected for an $S = 1/2$ radical (Figure 4).

2.2. Oxidation of Diaryldiamine and Aza[14]metacyclophane. Oxidations of diaryldiamine **5** and aza[14]metacyclophane **6** (Chart 1) with *m*-CPBA or DMDO, using similar conditions to those that gave good yields of diarylnitroxide radical **1**, resulted in complex mixtures, with no evidence for the corresponding diradical or the tetradical. To solve this problem, we developed a method for oxidation of diarylamines to nitroxides at low temperature, with the EPR, EPR/SQUID/EPR,^{37,38} and ^1H NMR/EPR monitoring of the reaction mixtures.

2.2.1. EPR Monitoring. First, we determined that oxidation of diarylamine **4** with DMDO (2–2.5 equiv) in dichloromethane at -95 or $-78\text{ }^\circ\text{C}$ gives intense EPR spectra for nitroxide monoradical at 140 K (Figures S4A–C, Supporting Information). Using similar conditions (2–2.5 equiv of DMDO per NH moiety), oxidation of diaryldiamine **5** and aza[14]meta-

(37) Rajca, A.; Shiraishi, K.; Pink, M.; Rajca, S. *J. Am. Chem. Soc.* **2007**, *129*, 7232–7233.

(38) Rajca, A.; Shiraishi, K.; Vale, M.; Han, H.; Rajca, S. *J. Am. Chem. Soc.* **2005**, *127*, 9014–9020.

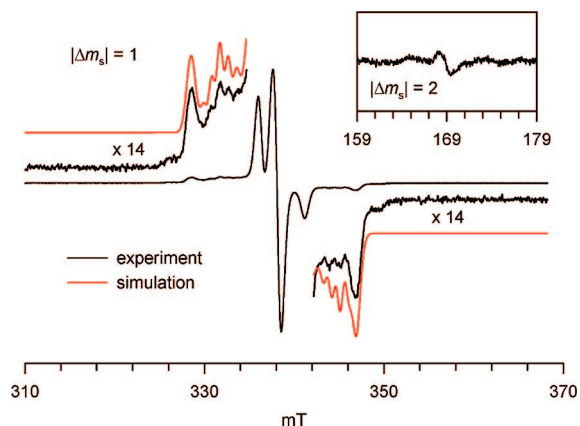
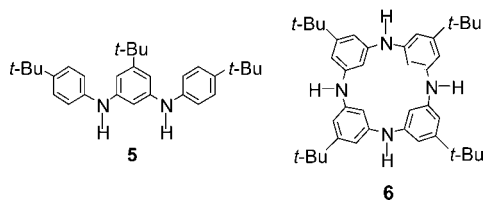


Figure 5. EPR (X-band, $\nu = 9.4875$ GHz, dichloromethane, 140 K) spectra for the reaction mixture obtained by oxidation of diaryldiamine **5** with DMDO at -90 °C. The simulation parameters for the $S = 1$ state are: $|D/hc| = 8.6 \times 10^{-3}$ cm $^{-1}$, $|E/hc| = 1.3 \times 10^{-3}$ cm $^{-1}$, $|A_{yy}/hc| = 8.5 \times 10^{-4}$ cm $^{-1}$, $g_x \approx 2.005$, $g_y = 2.0028$, $g_z = 2.0072$, Gaussian line ($L_x = 0.8$, $L_y = 0.65$, $L_z = 1.0$ mT). The center lines correspond to an $S = 1/2$ product.

Chart 1. Structures of diaryldiamine **5** and aza[1 $_4$]metacyclophane **6**

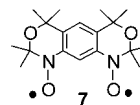


cyclophane **6** is monitored by EPR spectroscopy. The EPR spectra of frozen reaction mixtures derived from **5** and **6** show triplet-like center resonances of nitroxide monoradical that are flanked by weak side bands (Figure 5 and Figure S7, Supporting Information).

The EPR spectra for the reaction mixture obtained by oxidation of diaryldiamine **5** are better resolved. The side bands in EPR spectra at 140 K could be assigned to dipolar coupling patterns of two $S = 1$ diradicals **2**, presumably one major and one minor conformer, with smaller and larger spectral widths ($|2D/hc|$), respectively (Figure 5),^{28,39,40} based upon the relative values of $|2D/hc|$, the major and minor conformer are expected to possess longer and shorter interspin distances between nitroxides, respectively.⁴¹

For the major conformer of diradical **2**, the part of the experimental spectrum in the $|\Delta m_s| = 1$ region that is not obstructed by the intense $S = 1/2$ resonances can be reproduced by the simulated powder pattern for electron–electron dipolar coupling and ^{14}N -hyperfine coupling (Figure 5). The electron–electron dipolar coupling gives rise to two zero-field splitting (zfs) parameters: $|D/hc| = 8.6 \times 10^{-3}$ cm $^{-1}$ and $|E/hc| = 1.3 \times 10^{-3}$ cm $^{-1}$; the value of $|E|$ is a significant fraction of $|2D|$, thus indicating large deviation of spin density distribution from axial symmetry. The yy -component of the ^{14}N -hyperfine coupling

Chart 2. Structure of alkylarylnitroxide diradical **7**



appears as a pentuplet with significant splitting of $|A_{yy}/2hc| \approx 8.5 \times 10^{-4}$ cm $^{-1}$ and the corresponding value of $g_y = 2.0028$ is similar to the free-electron value of 2.0023. These spectral features suggest that the nitroxide moieties are approximately coplanar with the m -phenylene, or perhaps only slightly distorted from coplanarity.²⁰

For the minor conformer, only the outermost bands may be discerned, thus allowing only for determination of approximate value of $|D/hc| \approx 11 \times 10^{-3}$ cm $^{-1}$. As mentioned in the preceding paragraphs, this relatively large value of $|2D/hc|$ suggests smaller interspin distance in the minor conformer.

The side bands in EPR spectra for the reaction mixture obtained by oxidation of aza[1 $_4$]metacyclophane **6** are very weak, and thus it is most likely that they would correspond an $S = 1$ diradical. The value of $2D$ is similar to that for the major conformer of **2**. Spectral simulations of the $|\Delta m_s| = 1$ region, which is not overlapped with the intense $S = 1/2$ resonances, reproduce the experimental spectra with $|D/hc| = 8.9 \times 10^{-3}$ cm $^{-1}$ and $|E/hc| = 1.15 \times 10^{-3}$ cm $^{-1}$ (Figures S6A and S7, Supporting Information).

In diradical **2**, with approximately planar conformation, the spin density is likely to be significantly delocalized from the nitroxide moieties onto the m -phenylene and 4-*tert*-butylphenyls. This delocalization should lead to the relatively low value of ^{14}N -hyperfine coupling for **2**. In particular, the value of $|A_{yy}/hc| \approx 0.0017$ cm $^{-1}$ obtained from the spectral simulations in Figure 5 may be viewed as the lower limit for the largest principal value of the ^{14}N -hyperfine tensor.⁴² The value of $|A_{yy}/hc| \approx 0.0017$ cm $^{-1}$ for delocalized diarylnitroxide diradical **2** is significantly lower than the largest principal values of the ^{14}N -hyperfine tensor for planar alkylarylnitroxide diradical **7** (0.0024 cm $^{-1}$) (Chart 2),^{20,43} *tert*-butylarylnitroxide diradical (~ 0.0026 cm $^{-1}$),⁴⁴ and for localized di-*tert*-butylnitroxide radical (0.0030 cm $^{-1}$).⁴⁵

These EPR spectral analyses establish the presence of triplet state for diradical **2**. To determine whether the triplet state is the ground-state or the excited state, and to estimate concentration of the paramagnetic radicals, SQUID magnetic measurements were carried out.

2.2.2. EPR/SQUID/EPR Monitoring. Another set of oxidations of diaryldiamine **5** and aza[1 $_4$]metacyclophane **6** was carried out in homemade tubes that allow for handling of samples at strictly low temperature and direct EPR/SQUID/EPR monitoring of the reaction mixtures (Figures S10A–C and S11A–C, Supporting Information). DMDO was reacted with **5** and **6** at about -80 and -90 °C, respectively; EPR spectra

(39) Calder, A.; Forrester, A. R.; James, P. G.; Luckhurst, G. R. *J. Am. Chem. Soc.* **1969**, *91*, 3724–3727.

(40) Spagnol, G.; Shiraishi, K.; Rajca, S.; Rajca, A. *Chem. Commun.* **2005**, 5047–5049.

(41) (a) The dependence of the spectral width ($|2D|$) on the inter-dipole distance (r) is calculated according to the following equation: $|2D| = 3g\beta/r^3 = 2.78 \times 10^3 (g/r^3)$, where $|D|$ is in mT and r is in Å. (b) Eaton, S. S.; More, K. M.; Sawant, B. M.; Eaton, G. R. *J. Am. Chem. Soc.* **1983**, *105*, 6560–6567.

(42) In the spectral simulation of **2** in Figure 5, it is assumed that the magnetic dipole-dipole inter-spin vector (principal axis of the diradical D -tensor) is along a principal axis of the nitroxide g - and A -tensor. Out-of-plane distortion in **2** may misalign the principal axes, and thus the value of “ $|A_{yy}/hc|$ ” with the y -axis defined by the D -tensor in the spectral simulation would be lower, underestimating the actual value of $|A_{yy}/hc|$ with the y -axis parallel to the $2p_N$ orbital axis.

(43) Rassat, A.; Sieveking, U. *Angew. Chem., Int. Ed. Engl.* **1972**, *11*, 303–304.

(44) Griffith, O. H.; Cornell, D. W.; McConnell, H. M. *J. Chem. Phys.* **1965**, *43*, 2909–2910.

(45) Rajca, A.; Mukherjee, S.; Pink, M.; Rajca, S. *J. Am. Chem. Soc.* **2006**, *118*, 13497–13507.

similar to those obtained in the previous EPR monitoring experiments were obtained. SQUID magnetometry showed that the values of χT and M_{sat} are very low, indicating that the content of paramagnetic radicals is on the order of 1%, based upon the weight of the starting amines. The magnetization data plotted as M/M_{sat} vs H/T follow Brillouin functions with the value of $S = 1/2 - 1$, as expected for a mixture of $S = 1/2$ monoradical and $S = 1$ ground-state diradical. These magnetic data are consistent with the EPR spectra, which showed dominant center peaks ($S = 1/2$ monoradical) and much smaller side bands ($S > 1/2$ species, most likely, $S = 1$ diradical). For diradical **2**, the relative intensities of the side bands and the center peaks in the EPR spectra, taken before and after the SQUID magnetometry, are in qualitative agreement with the average values S obtained from the curvature of the M/M_{sat} vs H/T Brillouin plots.⁴⁶ In magnetic studies, the measurement of 1% content of paramagnetic radicals with the overwhelming diamagnetic component and organic solvent matrix is very difficult. Therefore, the similar molar ratio of the $S = 1$ diradical to $S = 1/2$ monoradical determined by EPR spectra and SQUID magnetometry is significant, as it precludes a possible contribution from paramagnetic metal impurities. Thus, diarylnitroxide diradical **2** possesses triplet ground state. However, the ground-state for the diradicals derived from aza[14]metacyclophane **6** could not be established, due to a relatively weak EPR signal for side bands.

Because the diamagnetic component is dominant in oxidations starting from **5** and **6**, the ^1H NMR/EPR monitoring experiments of the reaction mixtures were carried out.

2.2.3. ^1H NMR/EPR Monitoring. Oxidations of diaryldiamine **5** and aza[14]metacyclophane **6** with DMDO were carried out in flame sealed NMR sample tubes while the reaction progress was monitored by ^1H NMR and EPR spectroscopy (Figures S12A–E and Figures S13A–H, Supporting Information). For the reaction mixtures that are strictly handled at low temperature ($-78\text{ }^\circ\text{C}$ or lower temperature) for 1–4 h, resonances that may be assigned to the diamagnetic byproduct are observed. EPR spectra of such reaction mixtures at 140 K are similar to those observed for the reaction mixtures monitored by EPR and EPR/SQUID/EPR, including the presence of the side-bands, as described in the preceding paragraphs. When the reaction mixtures are allowed to attain room temperature, the integrations of the resonances that may be assigned to diamagnetic byproduct are significantly increased. The EPR spectra of such mixtures at 140 K show no side bands and only the center resonances assigned to nitroxide monoradicals are detectable. The EPR spectra at room temperature show resolved hyperfine patterns that are in qualitative agreement with the ^{14}N - and ^1H -hyperfine splittings that are expected for the nitroxide monoradicals **2-m** and **3-m**, formed by oxidation of diaryldiamine **5** and aza[14]metacyclophane **6**, respectively (Figure 6).

2.2.4. Conformers of Nitroxide Diradical 2: DFT Calculations and EPR Spectral Widths. Geometries for triplet states

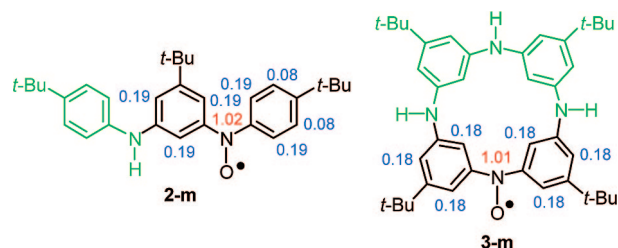


Figure 6. Structures for the nitroxide monoradicals **2-m** and **3-m** (drawing in black); the remaining parts of the structure, derived from diaryldiamine **5** and aza[14]metacyclophane **6** (drawn in green), are not detected in the EPR spectra and thus details of their structure are not known. The ^{14}N - and ^1H -hyperfine splittings (mT) are shown in red and blue, respectively. EPR spectra and spectral simulations are reported in Figures S8H and S9E in the Supporting Information.

of three limiting conformers of diradical **2** are fully optimized at the UB3LYP/6-31G(d) level (Table 1).⁴⁷ Vibrational frequency calculations indicate that all three conformers are local minima on the potential energy surface. In all three conformers, the torsional angles (α and β , or $180 - \alpha$ and $180 - \beta$) between the nitroxide and *m*-phenylene moieties are in the $25\text{--}29^\circ$ range. All three conformers are triplet ground states with the singlet–triplet energy gaps of 1.5–1.8 kcal/mol, as expected for a moderately twisted *m*-phenylene-based nitroxide diradicals.¹⁷

The triplet ground states of **2A-anti**, **2B-endo**, and **2C-exo** are within only 1.1 kcal mol^{-1} , thus not allowing for a conclusive assignment of the major conformer observed in the EPR spectra in the condensed phase. For example, the relative energies of **2A-anti**, **2B-endo**, and **2C-exo** in polar matrices, such as dichloromethane, may change significantly, as the conformers with the higher energies possess considerably larger dipole moments.^{39,40}

A tentative assignment of the major conformer and the minor conformer for diradical **2** is possible using the experimental values of $|2D/hc|$ (Figure 5) and their approximate relationship with the interspin distance.⁴¹ Conformationally constrained alkylarylnitroxide diradical **7** (Chart 2),^{20,43} which possesses planar structure with an interspin distance of 4.8 Å between the midpoints of the NO bonds, provides a well-characterized reference structure for conformer **2B-endo**. The measured value of $|2D/hc| = 2.7 \times 10^{-2}\text{ cm}^{-1}$ for **7** corresponds to the interspin distance of 5.8 Å; as expected for a diradical with delocalized spin density, the point-dipole approximation overestimates interspin distance, defined as average of N...N and O...O distances. This overestimate is expected to exceed 1 Å for more delocalized diarylnitroxide diradical **2**. The observed values of $|2D/hc| = 1.72 \times 10^{-2}\text{ cm}^{-1}$ and $|2D/hc| = 2.2 \times 10^{-2}\text{ cm}^{-1}$ for major and minor conformers correspond to the interspin distances of 6.7 Å and 6.2 Å, respectively. These distances are overestimated by 1.1–1.3 Å compared to the calculated averages of N...N and O...O distances in **2A-anti** and **2B-**

(46) (a) For oxidations of diaryldiamine **5**, the relative EPR signal intensities from double integration of the side bands and the center peaks are about 0.3: 0.7, respectively (Figures S5A and S5C, Supporting Information). Because the side-bands underneath the center peaks could not be integrated and the EPR intensities are related by a factor of $S(S+1)$, the ratio of 0.3: 0.7 is probably not much different from the molar ratio of $S = 1$ diradical to $S = 1/2$ monoradical. This ratio would give spin-average of S close to $S_s \approx 0.7$, which is in agreement with $S = 1/2 - 1$ obtained from the curvature of Brillouin plots (Figure S5B, Supporting Information). (b) S_s is approximately related to the curvature of Brillouin plots. Rajca, A.; Rajca, S.; Wongsriratanakul, J. *J. Am. Chem. Soc.* **1999**, *121*, 6308–6309.

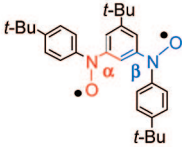
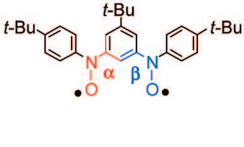
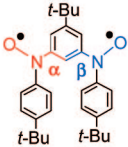
(47) Frisch, M. J.; et al. *Gaussian 03*; Gaussian, Inc.: Wallingford CT, 2004.

(48) Full geometry optimization of the broken-symmetry singlet for **2A-anti** lowers the energy by 0.08 kcal mol⁻¹ only, thus the singlet geometries of were not optimized. This may introduce an additional, though small, source of overestimate of the singlet–triplet gaps.

(49) Zhang, D. Y.; Hrovat, D. A.; Abe, M.; Borden, W. T. *J. Am. Chem. Soc.* **2003**, *125*, 12823–12828.

(50) (a) Cramer, C. J.; Smith, B. A. *J. Phys. Chem.* **1996**, *100*, 9664–9670. (b) Winter, A. H.; Falvey, D. E.; Cramer, C. J.; Gherman, B. F. *J. Am. Chem. Soc.* **2007**, *129*, 10113–10119.

Table 1. UB3LYP/6-31G(d) Calculations for Conformers of Diradical 2

	2A-anti	2B-endo	2C-exo
Optimized geometry for triplets			
N...N, O...O distances (Å) for triplets	4.9, 6.2	4.8, 4.9	4.9, 7.0
α , β torsion angles (°) for triplets	25.2, 154.3	26.6, 26.3	-151.5, -151.7
Dipole moment ^a for triplets	2.87	5.51	3.42
Total energy for triplets (¹ E) ^b	-1425.92486953	-1425.92309079	-1425.92419925
Relative energy for triplets ^c	0	1.11	0.42
Zero-point-energy (ZPE) for triplets ^c	388.646	388.589	388.656
Total energy for BS singlets (^S E _{BS}) ^{b,d,e}	-1425.92343452	-1425.92187961	-1425.92287864
Singlet-triplet energy gap, 2(^S E _{BS} - ¹ E) ^{c,e}	1.8	1.5	1.7

^a Dipole moment in Debye. ^b In Hartree/molecule. ^c In kcal mol⁻¹. ^d Broken-symmetry singlet with $S(S+1) \approx 1.0$ at the geometry optimized for the triplet.⁴⁸⁻⁵⁰ ^e Full geometry optimization of the broken-symmetry singlet for **2A-anti** lowers the energy by 0.08 kcal mol⁻¹ only. The UB3LYP (broken symmetry with $S(S+1) \approx 1.0$ singlets and $S(S+1) \approx 2.0$ triplets) level of theory usually overestimates the singlet-triplet gaps, $2(^S E_{BS} - ^1 E)$, for the triplet ground state organic diradicals, and underestimates such gaps for the singlet ground state diradicals.^{49,50}

endo, respectively. An alternative assignment of the minor conformers to **2A-anti** and the major conformer to **2C-exo** would lead to an overestimate of about 0.6 – 0.7 Å, too low for delocalized *m*-phenylene diarylnitroxide diradicals. Therefore, we conclude that **2A-anti** corresponds to the major conformer of **2**.

3. Experimental Section

3.1. Materials. Amine **4** and diamine **5** were prepared using Pd-catalyzed aminations as described in the Supporting Information. Aza[1₄]metacyclophane **6** was prepared using recently reported procedure.³⁰ Amines were oxidized to nitroxide radicals using dimethyldioxirane (DMDO) or *m*-chloroperbenzoic acid (*m*-CPBA) using the following procedures.

3.2. 3,2, 4,4-Di-tert-butyl-diphenylnitroxide Radical 1. *m*-CPBA (22.4 mg, 0.130 mmol) in dry chloroform-*d* (1 mL) was added to a stirred solution of amine **4** (18.2 mg, 64.1 μmol) in dry chloroform-*d* (2 mL) at 0 °C over 5 min under nitrogen atmosphere. The reaction mixture turned orange immediately and was stirred for a further 30 min at 0 °C, and then was concentrated in vacuo to give an orange solid (35.0 mg). Preparative TLC (chloroform/hexanes, 60:40) produced **1** as an orange solid (18.0 mg, 74%). From two other reactions, 51.0 mg (63%) of **1** was obtained from 76.4 mg of amine **4**; the orange solid was combined and recrystallized from methanol (30 °C) to give two crops of deep orange crystals (46 mg, 57%) of nitroxide radical **1**.

In an alternative procedure, DMDO (0.06 M, 2 mL, 0.121 mmol, 2.2 equiv) in acetone at -20 °C was added to a solution of amine **4** (15.4 mg, 0.055 mmol, 1.0 equiv) in dichloromethane (5 mL) at -78 °C. The reaction mixture turned orange immediately and it was allowed to reach -20 °C over 1 h. The solvent and excess oxidant was removed in vacuo. The crude was extracted with chloroform, the organics were separated and dried over MgSO₄, and concentrated in vacuo to give an orange solid (17.8 mg). A

repeat reaction was carried was in acetone (5 mL), starting from 15.7 mg of amine **4**. The combined crude orange solids (31.1 mg) from the two reactions were purified by preparative TLC, followed by recrystallization (as described above), to give deep orange crystals (13.7 mg, 43%) of nitroxide radical **1**. In another reaction, 57.9 mg (60%) of nitroxide radical **1** was obtained from 90.0 mg of amine **4** in dichloromethane (10 mL) and 2.9 equiv of DMDO at -20 °C, after column chromatography and recrystallization from ethanol at 35 °C with cooling to either -20 or -78 °C. On the basis of ¹H NMR integration, the crystals of **1** contained about 10 mol % of solvent of crystallization (methanol or ethanol).

¹H NMR (300 MHz, chloroform-*d*): δ = 6.20 ppm (br s, 18 H), methanol solvent peak at 3.88 (0.25 H), impurities at 0.489 (0.22 H). EPR (X-band, 9.4229 GHz, 8×10^{-5} M, diethyl ether): hyperfine splitting in mT (number of nuclei), $a_N = 0.97$ (1), $a_H = 0.19$ (4), $a_{H'} = 0.08$ (4), 100% Lorentzian line width = 0.035 mT, $g \approx 2.005$, $R = 0.998$. IR (ZnSe, cm⁻¹): 2960, 2866, 1493, 1361, 1266, 830. EPR, ¹H NMR, and IR spectra are shown in Figures S1–S3 (Supporting Information).

3.3. General Procedure for EPR/SQUID/EPR and EPR Monitoring of Oxidation of Diarylamines at Low Temperature. Diarylamine **4**, diaryldiamine **5**, or aza[1₄]metacyclophane **6** (1–3 mg) was placed in the homemade SQUID tube (5-mm O.D. EPR quartz tube with a thin bottom ~6 cm from the end of the tube)^{47,48} or in the 4-mm O.D. EPR quartz tube equipped with high-vac PTFE stopcock, and then evacuated. Dichloromethane, followed by DMDO, were vacuum transferred to the vessel. The reaction mixture was stirred at specified temperature between -80 and -95 °C for specified periods, and then EPR spectra were obtained. After SQUID data were obtained, another set of EPR spectra were obtained. The EPR spectra that were obtained before and after the magnetic measurements were practically identical. The samples for magnetic measurements and EPR spectroscopy were handled at strictly low temperatures, using similar procedures that were previously developed for polyarylmethyl polyradicals.³⁸

3.4. General Procedure for ^1H NMR/EPR Monitoring of Oxidation of Diarylamines at Low Temperature. Diaryldiamine **5** or aza[14]metacyclophane **6** (3–6 mg) was placed in a 5-mm NMR tube (or custom-made 5-mm NMR tube transitioning in the lower part a 3-mm NMR tube) equipped with high-vac PTFE stopcock, and then evacuated. Dichloromethane- d_2 , followed by DMDO, were vacuum transferred to the vessel, and then the NMR tubes were flame-sealed. The reaction mixture was stirred at specified temperature between -80 and -95 °C for specified periods, and then the NMR tube was inserted to an NMR probe at about -87 °C. After obtaining ^1H NMR spectra, the sample was ejected cold from the probe, and then EPR spectra were obtained at low temperatures. Subsequently, the samples were allowed to attain room temperature, and ^1H NMR spectra at room temperature were obtained, as well as EPR spectra at low temperatures and at room temperature.

3.5. EPR Spectroscopy. CW X-band EPR spectra were acquired on an instrument, equipped with a frequency counter and nitrogen flow temperature control (130–300 K). The samples were contained in either the 5-mm quartz SQUID sample tubes or 4-mm quartz EPR sample tubes, which were either flame-sealed or closed with high-vac PTFE stopcocks. Typically, the tubes were inserted to the precooled cavity at 140 K. All spectra were obtained with the oscillating magnetic field perpendicular (TE_{102}) to the swept magnetic field. The g values were referenced using DPPH ($g = 2.0037$, powder).

3.6. SQUID Magnetometry. Quantum Design MPMS5S (with continuous temperature control) was used. All samples were contained in homemade SQUID tubes.^{51,52}

For solid state samples, polycrystalline **1** was obtained by crystallization from ethanol at 35 °C with cooling to -20 °C. Radical **1** was loaded to the SQUID tube, placed under vacuum, and then flame sealed under partial pressure of helium gas. Correction for diamagnetism was based upon high-temperature linear extrapolation of the M vs $1/T$ plots at 5000 Oe; the numerical fits in 270–90 K range ($R^2 = 1.0000$) gave intercept (M_{dia}), which was added to the magnetization at field H as a factor, $(M_{\text{dia}}H)/5000$. Analogous procedure for correction for diamagnetism was used for a sample in gelatine capsule. For solution sample of nitroxide radical **1** in 2-MeTHF, solid **1** (2.04 mg) was loaded to the tube, 2-MeTHF (0.05–0.07 mL) was vacuum transferred, and then the tube was flame-sealed under vacuum. The tube was inserted to the sample chamber of the magnetometer at 290 K; the initial sequence of measurements was in the cooling mode to allow for condensation of 2-MeTHF. Correction for diamagnetism was based

upon high temperature linear extrapolation of the M vs $1/T$ plots, using numerical fits in 200–70 K range ($R^2 = 1.0000$, cooling mode).

3.7. EPR Spectral Simulations and Numerical Curve Fitting for SQUID Magnetic Data. WinSIM program (Public EPR Software Tools, D. A. O'Brien, D. R. Duling, Y. C. Fann) and WINEPR SimFonia program (Version 1.25) were used for EPR spectral simulations of solution phase spectra and rigid matrix spectra, respectively. The SigmaPlot software package was used for numerical curve fitting of magnetic data. The reliability of fit is measured by the parameter dependence, which is defined as follows: $\text{dependence} = 1 - ((\text{variance of the parameter, other parameters constant})/(\text{variance of the parameter, other parameters changing}))$. Values close to 1 indicate overparametrized fit.

4. Conclusions

In polycrystalline diarylnitroxide radical **1**, weak intermolecular ferromagnetic interactions are determined by magnetic susceptibility and magnetization studies. Our low-temperature procedure for oxidation of diarylamine allowed us to detect for the first time the *m*-phenylene-based diarylnitroxide diradical. EPR spectroscopy and magnetic studies (SQUID) indicate that diarylnitroxide diradical **2** in frozen dichloromethane is observed in predominantly anti conformation (**2A-anti**) and it possesses triplet ground state. Similar oxidation experiments for aza[14]metacyclophane provide evidence for the formation of small amounts of the corresponding diarylnitroxide diradical.

It appears that diarylnitroxide diradicals are much less stable than their corresponding alkylarylnitroxide diradicals, as well as diarylnitroxide monoradicals. This may imply that steric shielding of *m*-phenylene by a 5-*tert*-butyl group is insufficient and steric shielding of all para positions with respect to nitroxides may be required for stable *m*-phenylene-based diarylnitroxide diradicals.

Acknowledgment. This research was supported by the National Science Foundation (CHE-0107241, CHE-0414936, CHE-0718117), including the purchase of the Electron Paramagnetic Resonance (EPR) spectrometer used in this work (DMR-0216788).

Supporting Information Available: Materials and general procedures, experimental details (routine analyses, EPR, EPR/SQUID/EPR, EPR/ ^1H NMR monitoring data for preparation of nitroxide radicals, NMR spectra of synthetic intermediates), computational details, and complete ref 47. This material is available free of charge via the Internet at <http://pubs.acs.org>.

JA8016335

(51) Rajca, A.; Pink, M.; Rojsajakul, T.; Lu, K.; Wang, H.; Rajca, S. *J. Am. Chem. Soc.* **2003**, *125*, 8534–8538.

(52) Rajca, S.; Rajca, A.; Wongsriratanakul, J.; Butler, P.; Choi, S. *J. Am. Chem. Soc.* **2004**, *126*, 6972–6986.